

Molecule Edit Graph Attention Network: Modeling Chemical Reactions as Sequences of Graph Edits

Mikołaj Sacha,¹ Mikołaj Błaż,¹ Piotr Byrski,¹
Paweł Włodarczyk-Pruszyński,¹ Stanisław Jastrzębski^{1,2}

Abstract

One of the key challenges in automated synthesis planning is to generate diverse and reliable chemical reactions. Many reactions can be naturally represented using graph transformation rules referred broadly to as *reaction templates*. Using reaction templates enables accurate and interpretable predictions but can suffer from limited coverage of the reaction space. On the other hand, *template-free* methods can increase the coverage but can be prone to making trivial mistakes and are challenging to interpret. A promising idea for constructing more interpretable template-free models is to model a reaction as a sequence of graph edits of the substrates. We extend this idea to retrosynthesis and scale it up to large datasets. We propose Molecule Edit Graph Attention Network (MEGAN), a template-free neural model that encodes reaction as a sequence of graph edits. We achieve competitive performance on both retrosynthesis and forward synthesis and in particular state-of-the-art top-k accuracy for larger K values. Crucially, the latter shows excellent coverage of the reaction space of our model. In summary, MEGAN brings together the strong elements of template-free and template-based models and can be applied to both retro and forward synthesis tasks.

1 Introduction

Synthesis planning answers the question of *how* to make a given molecule. Due to the substantial size and complexity of the reaction space, synthesis planning is a demanding task even for skilled chemists and remains an important roadblock in the drug discovery process [Blakemore et al., 2018].

Computer-aided synthesis planning (CASP) methods aim to assist chemists in designing syntheses [Corey and Wipke, 1969, Segler et al., 2018, Coley et al., 2018a, Lee et al., 2019]. Designing synthesis can involve predicting reaction outcomes for a given set of possible substrates (*forward synthesis prediction*), or proposing reactions that can simplify a given target molecule (*retrosynthesis prediction*). A robust framework for generating reaction candidates could significantly increase the efficiency of synthesis planning systems. However, it has been reported that current methods suffer from either lack of reliability or small diversity in the proposed reactions [Davies, 2019, Molga et al., 2019].

Retrosynthesis prediction is particularly useful for finding plausible pathways leading to desirable molecules. Many of the recent approaches to retrosynthesis employ a static library of *reaction templates*. A reaction template encodes a graph transformation rule that enables generating reactions by applying the rule to input molecules. Such methods are highly interpretable and achieve strong performance [Dai et al., 2019]. However, template-based methods have some disadvantages. Perhaps the most pressing one is that due to the computational limits they require modeling reactions using a relatively small number of templates. This necessarily limits the size of the chemical reaction space accessible by such methods.

¹Molecule.one, Poland

²New York University, USA

The shortcomings of template-based methods have been addressed with the development of template-free models for reaction generation. In particular, modeling reaction generation as a machine translation task has led to promising results [Schwaller et al., 2019, Karpov et al., 2019]. This and related methods are still however often outperformed in retrosynthesis by template-based methods [Dai et al., 2019]. They have been also argued to be prone to making trivial mistakes [Molga et al., 2019].

Arguably, a more natural approach to reaction generation is to represent reaction as a sequence of graph edits. Bradshaw et al. [2018] models reaction as a sequence of bond removals and additions. However, their approach is limited to a certain subset of the chemical reaction space (reactions with linear chain topology) and forward synthesis. Do et al. [2019] models reaction as a set of operation on atom pairs. Similarly, their method cannot be readily applied to retrosynthesis due to the lack of support for atom addition.

In this work, we present the Molecule Edit Graph Attention Network (MEGAN). We propose an encoder-decoder model that generates a reaction as a sequence of graph edits. We include atom addition and bond removal in the action space to apply the model to the retrosynthesis tasks, where we achieve state-of-the-art results. Specifically, our two main contributions are as follows:

- We extend the idea to model reaction as a sequence edits to retrosynthesis prediction and scale it to large datasets. This required introducing a novel encoder-decoder architecture and an efficient training procedure that avoids the need to use reinforcement learning.
- We achieve competitive performance on retrosynthesis and competitive performance on forward synthesis as well as state-of-the-art top-k accuracy for large K values on all tested datasets. This serves as evidence that MEGAN achieves excellent coverage of the reaction space.

2 Related work

Computer-aided reaction prediction has a rich history [Todd, 2005]. Early approaches to generating reactions relied on manually crafted rules [Salatin and Jorgensen, 1980], which were difficult to apply to novel chemistry. Another family of methods use physical chemistry calculations [Zimmerman, 2013]. These methods are typically too computationally intensive to be used in synthesis planning software and can be complemented using statistical methods that learn from data.

Statistical approaches to predicting reactions and designing syntheses paths can be broadly categorized into template-based and template-free approaches. Template-based approaches use reaction rules or templates. These templates can be automatically mined from a database of known reactions [Law et al., 2009]. Machine-learning models have been subsequently used to select or rank most relevant templates [Wei et al., 2016, Segler et al., 2018]. Such models can be applied to assess reactivity of atoms to which reaction rules should be applied [Jin et al., 2017, Coley et al., 2018b]. An interesting alternative to this approach is to prioritize transformations that have already been applied to similar molecules [Coley et al., 2017]. Suitable set of templates combined with a well designated ranking model can achieve state-of-the-art performance on standard retrosynthesis benchmarks Dai et al. [2019].

Template-free methods for reaction prediction have been introduced by employing standard machine translation models to directly predict target SMILES strings from input SMILES strings [Weininger, 1988]. Such approaches can be used out-of-the box for both forward synthesis [Schwaller et al., 2018, 2019] and retrosynthesis [Liu et al., 2017, Karpov et al., 2019]. However, these models act as black-boxes; they do not provide reasoning behind their predictions and are not able to map atoms between the substrates and the product. They have also been shown to make some trivial mistakes [Molga et al., 2019].

Our work focuses on another class of template-free methods, which defines reaction generation as predicting target graph by sequentially modifying input graph. Such approach, while remaining template-free, can provide a greater interpretability of predictions, which are modeled as direct transformations on

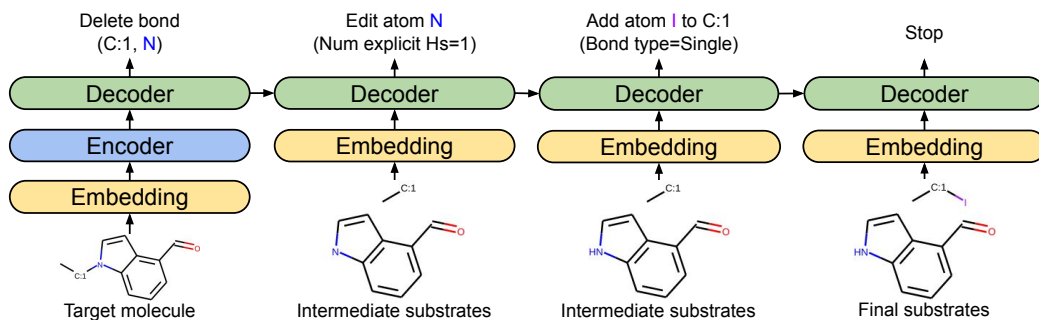


Figure 1: Retrosynthesis prediction generated by MEGAN. The model modifies the target molecule by sequentially executing actions on the molecular graph until it decides to stop.

molecules. Models that predict graph edits have been successfully applied to forward synthesis [Do et al., 2019] and can be fine-tuned to provide especially interpretable results on certain subsets of the chemical reaction space [Bradshaw et al., 2018]. In this work we propose a model inspired by these prior works and extend the approach to retrosynthesis prediction.

Concurrently to our work, the graph-edit reaction generation approach has been employed to retrosynthesis. The model presented in Shi et al. [2020] consists of two separate modules for predicting the reaction center and generating final substrates from the disconnected synthons. Somnath et al. [2020] employs a similar framework but completes the synthons with substructures which are selected from a predefined set found on the training data. Both of these approaches achieve high performance on a standard retrosynthesis benchmark. However, they are not shown to be scalable to larger datasets and are only evaluated for retrosynthesis prediction.

3 Molecule Edit Graph Attention Network

Graph Convolutional Networks (GCN) have been successfully applied to a variety of tasks in computational chemistry [Duvenaud et al., 2015, Xie and Grossman, 2018, You et al., 2018a, Coley et al., 2018b]. Our Molecule Edit Graph Attention Network (MEGAN) is an encoder-decoder architecture based on GCN that is able to predict a sequential series of actions on atoms and bonds of a chemical compound.

The key innovation is to combine an effective architecture and training procedure, which enables us to extend the ideas from Bradshaw et al. [2018], Do et al. [2019] to both retro and forward synthesis and achieve state of the art performance. We begin by describing the input and the output representation. Next, we introduce the overall architecture.

3.1 Input and output representation

We reformulate single-step reaction prediction as generating a series of actions on the graph of the input molecules that produce the graph of the output molecules. We define the following graph actions:

- Edit atom properties (*EditAtom*)
- Edit bond between two atoms (*EditBond*)
- Add new atom to the graph (*AddAtom*)
- Add new benzene ring to the graph (*AddBenzene*)

- Stop generation (*Stop*)

EditAtom changes properties of atoms, such as the formal charge, chirality or aromaticity. *EditBond* adds, edits or deletes a bond between two atoms. *AddAtom* adds a new atom of a specified type as a neighbor of another atom already existing in the graph, with a specified bond type. *AddBenzene* optimizes atom addition by appending a complete benzene ring to a selected carbon atom. *Stop* action indicates the end of the generation process. We use atom mapping information to define an order on actions, which we describe in the experimental section. We describe the possible actions in details in the Supplement.

Molecule representation MEGAN takes as input a molecular graph, which is represented by labeled node vectors and a labeled adjacency matrix. More specifically, the input consists of a matrix of features $H^{OH} \in \mathbb{Z}_{\geq 0}^{n \times h_{OH}}$ and an adjacency matrix $A^{OH} \in \mathbb{Z}_{\geq 0}^{n \times n \times a_{OH}}$, where n is the number of nodes in a graph and h_{OH} and a_{OH} are sizes of concatenated one-hot vectors of atom and bond features. Hydrogen atoms are removed from the graph, as for heavy atoms the number of neighboring hydrogen atoms can be deduced implicitly or marked explicitly by a special atom feature if needed. We select a minimal set of atom and bond features that allows for exact reconstruction of SMILES of all products and reactants from the development (training + validation) set. We describe the featurization in details in the Supplement.

3.2 Model architecture

First, input features are embedded using linear layers $f_{emb}: \mathbb{R}^{h_{OH}} \rightarrow \mathbb{R}^h$ and $g_{emb}: \mathbb{R}^{a_{OH}} \rightarrow \mathbb{R}^a$:

$$\mathbb{R}^{n \times h} \ni H^0 = f_{emb}(H^{OH}) \quad (1)$$

$$\mathbb{R}^{n \times n \times a} \ni A = g_{emb}(A^{OH}) \quad (2)$$

GCN-att layer The basic building block of the network is an attention-based GCN layer named *GCN-att*. We enhance the GCN layer from Veličković et al. [2017] by adding bond features as input information for computing the attention values. Let $H^t \in \mathbb{R}^{n \times h}$ denote input node features for the t -th GCN-att layer and $N(i) \subset \mathbb{Z}_{\geq 0}$ denote set of indices of neighbors of node at index i (where $i \in N(i)$). We calculate new node features $H^{t+1} \in \mathbb{R}^{n \times h}$ as follows:

$$\mathbb{R}^d \ni H_{i'}^t = \sigma_r(f_{att}^t(H_i^t)) \quad (3)$$

$$\mathbb{R}^{2d+a} \ni B_{ij}^t = H_{i'}^t \parallel H_{j'}^t \parallel A_{i,j} \quad (4)$$

$$\mathbb{R}^K \ni C_{ij}^t = f_{att'}^t(B_{ij}^t) \quad (5)$$

$$\mathbb{R}^h \ni G_{ik}^t = \sum_{j \in N(i)} \frac{\exp C_{ijk}^t}{\sum_{l \in N(i)} \exp C_{ilk}^t} H_j^t \quad (6)$$

$$\mathbb{R}^h \ni H_i^{t+1} = \parallel_{1 \leq k \leq K} \sigma_r(f_k^t(G_i^t)) \quad (7)$$

where σ_r denotes *relu* activation function, \parallel indicates vector concatenation, $K \in \mathbb{N}_+$ is the number of attention heads and $f_{att}: \mathbb{R}^h \rightarrow \mathbb{R}^d$, $f_{att'}: \mathbb{R}^{2d+a} \rightarrow \mathbb{R}^K$ and $f: \mathbb{R}^h \rightarrow \mathbb{R}^{h/K}$ are standard linear layers. Numbers h , a , d and K are hyperparameters of the model. We require that h is divisible by K . We use the same hyperparameter values for all GCN-att layers in the model but do not share their weights.

Supernode A single pass through a GCN-att layer transfers information only between neighboring atoms. This can potentially hinder the ability to learn graph-level features, such as coexistence of functional groups in different parts of a compound. To mitigate this, we introduce an additional node named *supernode* [Li et al., 2017], which is connected to all atoms in the graph with a special SUPERNODE bond type. Supernode is particularly useful for passing information between connected components of a graph, especially after it was split by deleting a bond.

Overall architecture The model consists of two parts: the *encoder*, which is invoked only once per reaction generation and the *decoder*, which is sequentially invoked to generate actions (Figure 3). The input graph is modified according to the predicted action at each step, until the *Stop* action is predicted. At each generation step, features of the intermediate graph are embedded using layers f_{emb} and g_{emb} . The encoder has N_e stacked GCN-att layers, which are invoked at the first generation step after the embedding layers. The decoder has N_d stacked GCN-att layers followed by final linear layers that output action probabilities for atom and bond actions as follows. Let $m = N_e + N_d$ for the first generation step and $m = N_d$ for the other generation steps. The logits L^a and L^b for atom actions Act_a and bond actions Act_b are calculated as follows:

$$\mathbb{R}^d \ni F_i = \sigma_r(g_{atom}(H_i^m)) \quad (8)$$

$$\mathbb{R}^{|Act_a|} \ni L_i^a = g'_{atom}(F_i) \quad (9)$$

$$\mathbb{R}^d \ni J_i = \sigma_r(g_{bond}(H_i^m)) \quad (10)$$

$$\mathbb{R}^{d+a} \ni J'_{ij} = \sigma_r(J_i + J_j \parallel A_{i,j}) \quad (11)$$

$$\mathbb{R}^{|Act_b|} \ni L_{ij}^b = g'_{bond}(J'_{ij}) \quad (12)$$

We reuse the hyperparameter value d for simplicity. To compute the final action probabilities, we apply softmax activation function to concatenated vectors of logits of all possible atom actions Act_a and possible bond actions Act_b . To decide which actions are legal, we use the following rules:

- *Stop* action can be predicted only by the supernode
- All other atom actions can be predicted by all nodes except the supernode.
- Bond actions can be predicted for indices i and j , where $i < j$ and nodes at i and j are atoms

We deliberately do not mask out redundant actions, such as deleting a non-existing bond or editing the atom to the same values of properties, as we expect the model to learn not to use such actions.

Retaining generation state Finally, we want our model to be *stateful*, that is to be able to take advantage of the information about the previous generation steps to predict the next action. We achieve this by storing the output H_s^m of the last GCN-att layer at the generation step s and merging it with the embedded input H_{s+1}^0 at step $s + 1$:

$$\mathbb{R}^h \ni H_{s+1}^0 := \max(H_{s+1}^0, H_s^m) \quad (13)$$

where \max is the piecewise maximum of vectors. In H_s^m , we zero-pad features for any node that was added to the graph at step s .

4 Experiments

We run experiments on standard benchmarks for retro and forward synthesis prediction. We begin by introducing the experimental setting.

4.1 Experimental setting

We evaluate the models on retro and forward synthesis prediction. The goal in retrosynthesis is to predict the set of reactants based on the product of a reaction. The goal in forward synthesis is to predict the product of a reaction based on the set of substrates. The accuracy is measured by comparing the SMILES [Weininger, 1988] representation of the predicted molecules to the SMILES representation of the ground truth target molecules. Before the comparison, we remove atom mapping information from the SMILES strings and canonicalize them using Rdkit [Landrum]. We use top-k accuracy computed on reactions from test set as the main evaluation metric.

Gradient-based training of MEGAN In contrast to Do et al. [2019] who use reinforcement learning to train their model, we back-propagate directly through the maximum likelihood objective to train MEGAN. This is nontrivial, as computing the gradient of the likelihood objective requires defining a fixed ordering of actions [You et al., 2018b]. To solve this issue, You et al. [2018b] enumerates atoms using breadth-first search. We adapt a similar idea to reaction generation. We use the mapping provided for reactions in the benchmark datasets, which describes atom correspondence between the product and the substrates to predetermine an ordering of actions. This provides supervision for each generation step and thus enables us to compute the gradient. We provide the remaining details in the Supplement.

Other training details of MEGAN For training, we use batch size of 4 reactions. We use Adam optimizer [Kingma and Ba, 2014] with the initial learning rate of 0.0001. We use warm-up, increasing the learning rate from 0 to 0.0001 over the first 20000 training steps. For efficiency, we compute the validation loss on a subset of 2500 validation samples after each 20000 training samples. We multiply the learning rate by 0.1 if the estimated validation loss has not decreased for more than 4 such validation checks. We stop the training after the estimated validation loss has not decreased for more than 8 validation checks. We adapt the hyperparameters based on the validation loss. The final hyperparameter values are described in the Supplement.

4.2 Results

We evaluate on three standard datasets for retro and forward synthesis prediction. We first evaluate on the standard retrosynthesis prediction benchmark USPTO-50k. Next, we investigate how MEGAN scales to large-scale retrosynthesis task. Finally, we present results on forward synthesis prediction on the USPTO-MIT dataset.

4.2.1 Retrosynthesis

Data First, we evaluate on the USPTO-50k dataset of approximately 50000 reactions, which was collected by Lowe [2012] and classified into 10 reaction types by Schneider et al. [2016]. We use the same processed version of the dataset as Coley et al. [2017], where each reaction consists of a single product molecule and a set of one or more reactants, with corresponding atoms between the reactants and the product mapped. Following other studies [Liu et al., 2017], we assign each reaction randomly to one of the training/validation/test sets with respective probabilities of 80%/10%/10%.

Table 1: Top-k test accuracy for retrosynthesis on the USPTO-50k dataset. Results of other methods taken from Dai et al. [2019] and Somnath et al. [2020]. † marks the concurrent work.

| METHODS | TOP-K ACCURACY % | | | | | |
|------------------------------|------------------|-------------|-------------|-------------|-------------|-------------|
| | 1 | 3 | 5 | 10 | 20 | 50 |
| REACTION TYPE UNKNOWN | | | | | | |
| TRANS | 37.9 | 57.3 | 62.7 | / | / | / |
| RETROSIM | 37.3 | 54.7 | 63.3 | 74.1 | 82.0 | 85.3 |
| NEURALSYM | 44.4 | 65.3 | 72.4 | 78.9 | 82.2 | 83.1 |
| G2Gs † | 48.9 | 67.6 | 72.5 | 75.5 | / | / |
| GLN | 52.5 | 69.0 | 75.6 | 83.7 | 89.0 | 92.4 |
| GRAPHRETRO † | 64.2 | 80.5 | 84.1 | 85.9 | / | 87.2 |
| MEGAN | 48.6 | 72.2 | 80.3 | 87.6 | 91.6 | 94.2 |
| REACTION TYPE GIVEN AS PRIOR | | | | | | |
| SEQ2SEQ | 37.4 | 52.4 | 57.0 | 61.7 | 65.9 | 70.7 |
| RETROSIM | 52.9 | 73.8 | 81.2 | 88.1 | 91.8 | 92.9 |
| NEURALSYM | 55.3 | 76.0 | 81.4 | 85.1 | 86.5 | 86.9 |
| G2Gs † | 61.0 | 81.3 | 86.0 | 88.7 | / | / |
| GLN | 64.2 | 79.1 | 85.2 | 90.0 | 92.3 | 93.2 |
| GRAPHRETRO † | 67.8 | 82.7 | 85.3 | 87.0 | / | 87.9 |
| MEGAN | 62.3 | 83.9 | 89.0 | 93.1 | 95.2 | 96.1 |

Experimental setting We run two variants of training on USPTO-50k: one with unknown reaction type and one for which reaction type is given as a prior by an additional embedding layer. For both runs, we use the same model architecture and the same training setup. The training takes approximately 16 hours on a single Nvidia Tesla K80 GPU for both variants.

We use beam search [Graves, 2012] on output probabilities of actions to generate multiple ranked candidates for each product. For USPTO-50k, we set the maximum number of steps to 16 and the beam width to 50, as it is the largest K for which accuracy was reported for the baseline models.

Baselines We compare performance of MEGAN on USPTO-50k with several template-free and template-based models, including current state-of-the-art methods. Seq2seq [Liu et al., 2017] and Transformer [Karpov et al., 2019] are both template-free methods based on machine translation models applied on SMILES strings. Retrosim [Coley et al., 2017] uses reaction fingerprint to select template based on similar reactions in the dataset. Neuralsym [Segler and Waller, 2017] uses a multi-linear perceptron to rank templates. GLN [Dai et al., 2019] employs a graph model that assesses when rules from templates should be applied.

We also compare MEGAN with two concurrently developed methods. G2G [Shi et al., 2020] is a template-free model based on modifying molecular graphs with a separate module for predicting reaction center. GraphRetro [Somnath et al., 2020] is a method similar to [Shi et al., 2020] that uses a discrete set of substructures for completing synthons.

Results Table 1 reports results on the USPTO-50k benchmark in a variant with and without reaction type information provided. We observe that the relative performance of MEGAN increases with growing values of K . For $K \geq 10$, MEGAN achieves state-of-the-art accuracy, outperforming all baselines in both settings.

We hypothesize that the advantage of MEGAN for large K stems largely from the fact that MEGAN

Table 2: Top-k test accuracy for retrosynthesis on the USPTO-FULL dataset. Results for other methods taken from Dai et al. [2019].

| | RETROSIM | NEURALSVM | GLN | MEGAN |
|--------|----------|-----------|-------------|-------------|
| TOP 1 | 32.8 | 35.8 | 39.3 | 33.6 |
| TOP 10 | 56.1 | 60.8 | 63.7 | 63.9 |
| TOP 50 | / | / | / | 74.1 |

generates reaction as a sequence of edits. This might help to efficiently search through different plausible reaction centers, hence covering a more diverse subset of the reaction space. It can also enable MEGAN to achieve high coverage of the reaction space, which is indicated by the top-50 accuracy of 94.2% when reaction type is unknown and 96.1% when reaction type is provided.

4.2.2 Large scale retrosynthesis prediction task

Data The USPTO-50k benchmark, although of relatively high quality, is a small dataset containing only 10 specific types of reactions. We train MEGAN for retrosynthesis on a large benchmark to test its scalability. We use the original data set collected by Lowe [2012] containing reactions from US patents dating from 1976 to September 2016. We use the same preprocessed and split data as Dai et al. [2019], which consists of approximately 800k/100k/100k training/validation/test reactions. We refer to this dataset as USPTO-FULL.

Experimental Setting We train MEGAN on USPTO-FULL using the same architecture and training procedure as for USPTO-50k. We only increase the maximum number of actions from 16 to 32 to account for more complex reactions in the dataset. We use beam search with beam width of 50 for evaluation. The training took about 60 hours on a single Tesla K80 GPU.

Results Table 2 shows top-k accuracy on USPTO-FULL for MEGAN compared to other methods for retrosynthesis prediction. We see that our model achieves competitive performance on a large scale retrosynthesis data set, slightly outperforming other methods in terms of top-10 accuracy.

4.2.3 Forward synthesis

Data Finally, we evaluate MEGAN on forward synthesis. We train the model on a standard forward synthesis benchmark of approximately 480000 atom-mapped chemical reactions, split into training/validation/test sets of 410k/30k/40k samples, which we call USPTO-MIT [Jin et al., 2017].

Baselines We compare MEGAN on forward synthesis with a few other methods. S2S [Schwaller et al., 2018] and MT [Schwaller et al., 2019] use machine translation models to predict the SMILES of the product from the SMILES of the substrates. WLDN [Jin et al., 2017] identifies pairwise atom interactions in the reaction center and ranks enumerated feasible bond configurations between these atoms. WLDN5 [Coley et al., 2018b] improves this method by combining the problems of reaction center prediction and candidate ranking into a single task. GTPN [Do et al., 2019] predicts actions on the graph of substrates, similarly to MEGAN, however limits them to actions between existing atom pairs.

Experimental Setting We remove the CHIRAL TAG and BOND STEREO features from the model input, as USPTO-MIT has no stereochemical information. Forward synthesis usually takes less modifications

Table 3: Top-1 test accuracy for forward synthesis on the USPTO-MIT dataset. Results for other methods taken from Schwaller et al. [2019].

| VARIANTS | S2S | WLDN | GTPN | WLDN5 | MT | MEGAN |
|-----------|------|------|------|-------|-------------|-------|
| SEPARATED | 80.3 | 79.6 | 82.4 | 85.6 | 90.4 | 89.3 |
| MIXED | | 74.0 | | | 88.6 | 86.3 |

Table 4: Top-k test accuracy of MEGAN and Molecular Transformer for forward synthesis on the USPTO-MIT dataset.

| METHODS | TOP-K ACCURACY % | | | | | |
|-----------|------------------|-------------|-------------|-------------|-------------|-------------|
| | 1 | 2 | 3 | 5 | 10 | 20 |
| SEPARATED | | | | | | |
| MT | 90.5 | 93.7 | 94.7 | 95.3 | 96.0 | 96.5 |
| MEGAN | 89.3 | 92.7 | 94.4 | 95.6 | 96.7 | 97.5 |
| MIXED | | | | | | |
| MT | 88.7 | 92.1 | 93.1 | 94.1 | 94.9 | 95.4 |
| MEGAN | 86.3 | 90.3 | 92.4 | 94.0 | 95.4 | 96.6 |

and is simpler to predict than retrosynthesis, so we reduce the maximum number of steps to 8 and use beam size of 20 for evaluation. We also change the train action ordering from *BFS rand-at* to *DFS cano-at* (see Section 4.3.1), as it demonstrates better validation performance for forward synthesis. Apart from these changes, we use the same architecture and training procedure as for USPTO-50k.

Similarly to Schwaller et al. [2019], we train for two variants of forward synthesis prediction. For the *separated* variant, compounds that directly contribute to the product are explicitly marked in the set of substrates with an additional atom feature. For the *mixed* variant, such information is not provided, so the model has a harder task as it has to determine the reaction center from a larger number of possible reactants.

Results Table 3 shows how MEGAN compares with other methods on both variants in terms of top-1 accuracy. In contrast to retrosynthesis, MEGAN is slightly outperformed by Molecular Transformer [Schwaller et al., 2019] on both forward synthesis tasks with the test accuracy of 89.3% for *separated* and 86.3% for *mixed*. This might be attributable to the larger difficulty of predicting atom mapping in the forward direction than in the backward direction, especially for the *mixed* variant. In contrast to Molecular Transformer, MEGAN predicts both the product molecule and the mapping between the substrates and the product; however, the atom mapping is not evaluated.

In Table 4 we compare the performance of MEGAN and Molecular Transformer on USPTO-MIT in top K predictions. We use the best non-ensemble models provided by Schwaller et al. [2019] and set the beam size to 20 during evaluation. We observe that MEGAN surpasses accuracy of Molecular Transformer for high K values, which again indicates its ability to explore the reaction space efficiently.

4.3 Analysis and ablation studies

4.3.1 Ablation study on action ordering

First, we investigate the importance of the action ordering using in training of MEGAN. To this end, we train MEGAN on USPTO-50k with a few methods of action ordering on the train set to investigate how

Table 5: Top-k test accuracy on USPTO-50k (reaction type unknown) for different methods of ordering actions on the train set.

| ACTION ORDER | TOP-K ACCURACY % | | | | | |
|--------------|------------------|-------------|-------------|-------------|-------------|-------------|
| | 1 | 3 | 5 | 10 | 20 | 50 |
| DFS CANO-AT | 47.6 | 71.2 | 79.5 | 87.0 | 91.4 | 94.2 |
| BFS CANO-AT | 47.5 | 71.8 | 80.2 | 87.0 | 91.4 | 94.5 |
| DFS RAND-AT | 43.9 | 67.9 | 76.4 | 83.8 | 88.4 | 92.4 |
| BFS RAND-AT | 48.6 | 72.2 | 80.3 | 87.6 | 91.6 | 94.2 |
| RANDOM | 44.0 | 61.7 | 69.8 | 78.5 | 84.4 | 89.5 |

it affects performance of the model. When generating training samples for a reaction, we store a list of atoms that have been edited or added. When choosing the next action, we prioritize atoms from this list. We compare two types of selecting the next atom from the list: DFS, where we prioritize the most recently inserted atoms and BFS, where we prioritize the least recently inserted atoms. For both variants, we test two methods of prioritizing unedited atoms in case there are no valid actions for atoms in the list: random priority of atoms (*rand-at*) or prioritizing atoms according to their order in the canonical smiles of target substrates from RdKit (*cano-at*). We also test a variant where the next action is simply taken randomly from the set of all possible actions (*random*). For all variants except for *random*, we use the canonical priority of action types, which we present in the Supplement. We present test top-k for all variants on USPTO-50k in Table 5. *BFS rand-at* ordering achieves the highest performance across most values of K , which motivates our choice to use it for training MEGAN on retrosynthesis prediction tasks.

4.3.2 Analysis of MEGAN predictions

Next, we analyse reactions generated by MEGAN in terms of their diversity and their popularity in the dataset. To approximate reaction popularity, we count the number of times that the corresponding template occurred in the training set. We use code provided by Coley et al. [2018b] to extract templates for each ground-truth reaction from the datasets, as well as for reactions predicted by MEGAN. To understand diversity of the proposed reaction, we extract reaction templates from the prediction and calculate the number of unique templates for a given K (the number of generated ranked reactions).

Figure 2 compares test accuracy of MEGAN and Molecular Transformer depending on the ground-truth reaction type popularity. We use the model provided by Karpov et al. [2019] to get Transformer predictions on USPTO-50k and results from Schwaller et al. [2019] for comparison on USPTO-MIT. We observe that MEGAN performs better on popular types of reactions and underperforms compared to Molecular Transformer on the most rare reactions. A natural topic for the future work is to improve performance of MEGAN on this subset of the reaction space.

Figure 3 shows diversity of reaction types predicted by MEGAN with respect to increasing K . The red curve shows the number of unique templates that could be matched to the proposed reactions. The blue curve shows how many of these unique templates were unseen in the training dataset.

First, we observe that MEGAN achieves a near linear relation between the number of proposed templates and the growing K . We also notice that MEGAN outputs reactions that do not fit any template seen in the train set. This is especially noticeable for forward synthesis, where most of the predictions do not fit any train template. These two observations suggest that MEGAN effectively searches through the chemical space of plausible reactions, which helps explain its strong performance at large K .

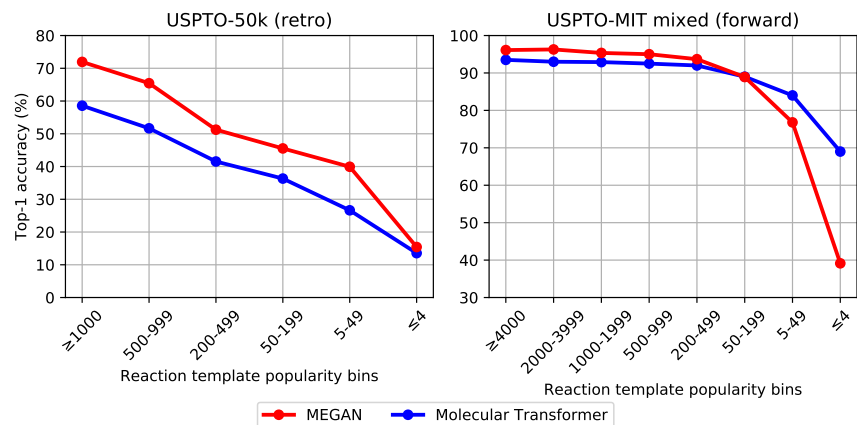


Figure 2: Top-1 test accuracy of MEGAN and Molecular Transformer with respect to the ground-truth reaction template popularity. MEGAN demonstrates relatively better performance on more popular reaction types.

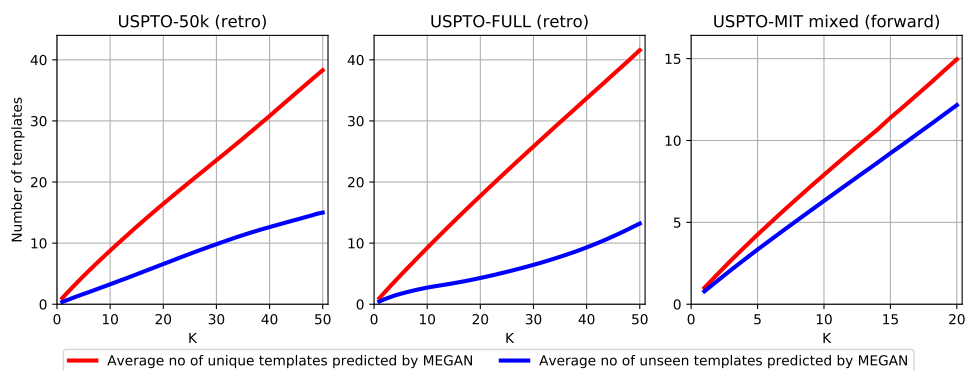


Figure 3: Average number of unique templates matching reactions predicted by MEGAN, combined with the number of predicted reaction types that do not fit any template seen on the train set. MEGAN utilizes beam search to search through space of plausible reaction types, including rare kinds of transformations.

5 Conclusions

In this work, we presented the Molecule Edit Graph Attention Network (MEGAN), a template-free model for both retrosynthesis and forward synthesis. We achieve competitive performance on retrosynthesis and forward synthesis as well as state-of-the-art top-k accuracy for large K values on all tested datasets. We also show that MEGAN can be scaled to large reaction datasets.

Crucially, MEGAN generates reaction as a sequence of graph edits. This inductive bias might explain the strong empirical performance of the model. In particular, we argued that it enables the model to more efficiently search through the space of plausible reactions. Looking forward, generating reactions as

a sequence of edits is promising for building more intuitive human-computer interaction in synthesis planning software.

A natural topic for the future is reducing the reliance of MEGAN on mapping between products and substrates. We also found that MEGAN under-performs for the most rare reactions in comparison to other models. Improving these two aspects has the potential to further push state-of-the-art in retro and forward synthesis prediction.

References

- David C. Blakemore, Luis Castro, Ian Churcher, David C. Rees, Andrew W. Thomas, David M. Wilson, and Anthony Wood. Organic synthesis provides opportunities to transform drug discovery. *Nature Chemistry*, 10(4):383–394, 2018. doi: 10.1038/s41557-018-0021-z. URL <https://doi.org/10.1038/s41557-018-0021-z>.
- John Bradshaw, Matt J. Kusner, Brooks Paige, Marwin H. S. Segler, and José Miguel Hernández-Lobato. A generative model for electron paths, 2018. URL <https://arxiv.org/abs/1805.10970>.
- Connor W. Coley, Luke Rogers, William H. Green, and Klavs F. Jensen. Computer-assisted retrosynthesis based on molecular similarity. *ACS Central Science*, 3(12):1237–1245, 2017. doi: 10.1021/acscentsci.7b00355. URL <https://doi.org/10.1021/acscentsci.7b00355>. PMID: 29296663.
- Connor W. Coley, William H. Green, and Klavs F. Jensen. Machine learning in computer-aided synthesis planning. *Accounts of Chemical Research*, 51(5):1281–1289, 2018a. doi: 10.1021/acs.accounts.8b00087. URL <https://doi.org/10.1021/acs.accounts.8b00087>. PMID: 29715002.
- Connor W. Coley, Wengong Jin, Luke Rogers, Timothy F. Jamison, Tommi S Jaakkola, William H. Green, Regina Barzilay, and Klavs F. Jensen. A graph-convolutional neural network model for the prediction of chemical reactivity, Oct 2018b. URL https://chemrxiv.org/articles/A_Graph_Convolutional_Neural_Network_Model_for_the_Prediction_of_Chemical_Reactivity/7163189/1.
- E. J. Corey and W. Todd Wipke. Computer-assisted design of complex organic syntheses. *Science*, 166(3902):178–192, 1969. ISSN 0036-8075. doi: 10.1126/science.166.3902.178. URL <https://science.sciencemag.org/content/166/3902/178>.
- Hanjun Dai, Chengtao Li, Connor Coley, Bo Dai, and Le Song. Retrosynthesis prediction with conditional graph logic network. In H. Wallach, H. Larochelle, A. Beygelzimer, F. d'Alché-Buc, E. Fox, and R. Garnett, editors, *Advances in Neural Information Processing Systems 32*, pages 8872–8882. Curran Associates, Inc., 2019. URL <http://papers.nips.cc/paper/9090-retrosynthesis-prediction-with-conditional-graph-logic-network.pdf>.
- Ian W. Davies. The digitization of organic synthesis. *Nature*, 570(7760):175–181, 2019. doi: 10.1038/s41586-019-1288-y. URL <https://doi.org/10.1038/s41586-019-1288-y>.
- Kien Do, Truyen Tran, and Svetha Venkatesh. Graph transformation policy network for chemical reaction prediction. In *Proceedings of the 25th ACM SIGKDD International Conference on Knowledge Discovery & Data Mining, KDD '19*, page 750–760, New York, NY, USA, 2019. Association for Computing Machinery. ISBN 9781450362016. doi: 10.1145/3292500.3330958. URL <https://doi.org/10.1145/3292500.3330958>.

- David K Duvenaud, Dougal Maclaurin, Jorge Iparraguirre, Rafael Bombarell, Timothy Hirzel, Alan Aspuru-Guzik, and Ryan P Adams. Convolutional networks on graphs for learning molecular fingerprints. In C. Cortes, N. D. Lawrence, D. D. Lee, M. Sugiyama, and R. Garnett, editors, *Advances in Neural Information Processing Systems 28*, pages 2224–2232. Curran Associates, Inc., 2015. URL <http://papers.nips.cc/paper/5954-convolutional-networks-on-graphs-for-learning-molecular-fingerprints.pdf>.
- Alex Graves. Sequence transduction with recurrent neural networks, 2012.
- Wengong Jin, Connor W. Coley, Regina Barzilay, and Tommi Jaakkola. Predicting organic reaction outcomes with weisfeiler-lehman network, 2017.
- Pavel Karpov, Guillaume Godin, and Igor Tetko. *A Transformer Model for Retrosynthesis*, pages 817–830. 09 2019. ISBN 978-3-030-30492-8. doi: 10.1007/978-3-030-30493-5_78.
- Diederik P. Kingma and Jimmy Ba. Adam: A method for stochastic optimization, 2014. URL <http://arxiv.org/abs/1412.6980>. cite arxiv:1412.6980Comment: Published as a conference paper at the 3rd International Conference for Learning Representations, San Diego, 2015.
- Greg Landrum. Rdkit: Open-source cheminformatics. URL <http://www.rdkit.org>.
- James Law, Zsolt Zsoldos, Aniko Simon, Darryl Reid, Yang Liu, Sing Yoong Khew, A. Peter Johnson, Sarah Major, Robert A. Wade, and Howard Y. Ando. Route designer: A retrosynthetic analysis tool utilizing automated retrosynthetic rule generation. *Journal of Chemical Information and Modeling*, 49(3): 593–602, 03 2009. doi: 10.1021/ci800228y. URL <https://doi.org/10.1021/ci800228y>.
- Alpha A. Lee, Qingyi Yang, Vishnu Sresht, Peter Bolgar, Xinjun Hou, Jacquelyn L. Klug-McLeod, and Christopher R. Butler. Molecular transformer unifies reaction prediction and retrosynthesis across pharma chemical space. *Chem. Commun.*, 55:12152–12155, 2019. doi: 10.1039/C9CC05122H. URL <http://dx.doi.org/10.1039/C9CC05122H>.
- Junying Li, Deng Cai, and Xiaofei He. Learning graph-level representation for drug discovery, 2017.
- Bowen Liu, Bharath Ramsundar, Prasad Kawthekar, Jade Shi, Joseph Gomes, Quang Luu Nguyen, Stephen Ho, Jack Sloane, Paul Wender, and Vijay Pande. Retrosynthetic reaction prediction using neural sequence-to-sequence models, 2017.
- Daniel Lowe. *Extraction of chemical structures and reactions from the literature*. PhD thesis, University of Cambridge, 10 2012. URL <https://www.repository.cam.ac.uk/handle/1810/244727>.
- Karol Molga, Ewa P. Gajewska, Sara Szymkuć, and Bartosz A. Grzybowski. The logic of translating chemical knowledge into machine-processable forms: a modern playground for physical-organic chemistry. *React. Chem. Eng.*, 4:1506–1521, 2019. doi: 10.1039/C9RE00076C. URL <http://dx.doi.org/10.1039/C9RE00076C>.
- Timothy D. Salatin and William L. Jorgensen. Computer-assisted mechanistic evaluation of organic reactions. 1. overview. *The Journal of Organic Chemistry*, 45(11):2043–2051, 05 1980. doi: 10.1021/jo01299a001. URL <https://doi.org/10.1021/jo01299a001>.
- Nadine Schneider, Nikolaus Stiefl, and Gregory A. Landrum. What’s what: The (nearly) definitive guide to reaction role assignment. *Journal of Chemical Information and Modeling*, 56(12):2336–2346, 2016. doi: 10.1021/acs.jcim.6b00564. URL <https://doi.org/10.1021/acs.jcim.6b00564>. PMID: 28024398.

- Philippe Schwaller, Théophile Gaudin, Dávid Lányi, Costas Bekas, and Teodoro Laino. “found in translation”: predicting outcomes of complex organic chemistry reactions using neural sequence-to-sequence models. *Chem. Sci.*, 9:6091–6098, 2018. doi: 10.1039/C8SC02339E. URL <http://dx.doi.org/10.1039/C8SC02339E>.
- Philippe Schwaller, Teodoro Laino, Théophile Gaudin, Peter Bolgar, Christopher A. Hunter, Costas Bekas, and Alpha A. Lee. Molecular transformer: A model for uncertainty-calibrated chemical reaction prediction. *ACS Central Science*, 5(9):1572–1583, Aug 2019. ISSN 2374-7951. doi: 10.1021/acscentsci.9b00576. URL <http://dx.doi.org/10.1021/acscentsci.9b00576>.
- Marwin H. S. Segler and Mark P. Waller. Neural-symbolic machine learning for retrosynthesis and reaction prediction. *Chemistry – A European Journal*, 23(25):5966–5971, 2017. doi: 10.1002/chem.201605499. URL <https://chemistry-europe.onlinelibrary.wiley.com/doi/abs/10.1002/chem.201605499>.
- Marwin H. S. Segler, Mike Preuss, and Mark P. Waller. Planning chemical syntheses with deep neural networks and symbolic ai. *Nature*, 555(7698):604–610, 2018. doi: 10.1038/nature25978. URL <https://doi.org/10.1038/nature25978>.
- Chence Shi, Minkai Xu, Hongyu Guo, Ming Zhang, and Jian Tang. A graph to graphs framework for retrosynthesis prediction, 2020.
- Vignesh Ram Somnath, Charlotte Bunne, Connor W. Coley, Andreas Krause, and Regina Barzilay. Learning graph models for template-free retrosynthesis, 2020.
- Matthew H. Todd. Computer-aided organic synthesis. *Chem. Soc. Rev.*, 34:247–266, 2005. doi: 10.1039/B104620A. URL <http://dx.doi.org/10.1039/B104620A>.
- Petar Veličković, Guillem Cucurull, Arantxa Casanova, Adriana Romero, Pietro Liò, and Yoshua Bengio. Graph attention networks, 2017.
- Jennifer N. Wei, David Duvenaud, and Alán Aspuru-Guzik. Neural networks for the prediction of organic chemistry reactions. *ACS Central Science*, 2(10):725–732, 10 2016. doi: 10.1021/acscentsci.6b00219. URL <https://doi.org/10.1021/acscentsci.6b00219>.
- David Weininger. Smiles, a chemical language and information system. 1. introduction to methodology and encoding rules. *Journal of Chemical Information and Computer Sciences*, 28(1):31–36, 1988. doi: 10.1021/ci00057a005. URL <https://pubs.acs.org/doi/abs/10.1021/ci00057a005>.
- Tian Xie and Jeffrey C. Grossman. Crystal graph convolutional neural networks for an accurate and interpretable prediction of material properties. *Phys. Rev. Lett.*, 120:145301, Apr 2018. doi: 10.1103/PhysRevLett.120.145301. URL <https://link.aps.org/doi/10.1103/PhysRevLett.120.145301>.
- Jiaxuan You, Bowen Liu, Zhitao Ying, Vijay Pande, and Jure Leskovec. Graph convolutional policy network for goal-directed molecular graph generation. In S. Bengio, H. Wallach, H. Larochelle, K. Grauman, N. Cesa-Bianchi, and R. Garnett, editors, *Advances in Neural Information Processing Systems 31*, pages 6410–6421. Curran Associates, Inc., 2018a. URL <http://papers.nips.cc/paper/7877-graph-convolutional-policy-network-for-goal-directed-molecular-graph-generation.pdf>.
- Jiaxuan You, Rex Ying, Xiang Ren, William Hamilton, and Jure Leskovec. GraphRNN: Generating realistic graphs with deep auto-regressive models. In Jennifer Dy and Andreas Krause, editors,

Proceedings of the 35th International Conference on Machine Learning, volume 80 of *Proceedings of Machine Learning Research*, pages 5708–5717, Stockholmsmässan, Stockholm Sweden, 10–15 Jul 2018b. PMLR. URL <http://proceedings.mlr.press/v80/you18a.html>.

Paul M. Zimmerman. Automated discovery of chemically reasonable elementary reaction steps. *Journal of Computational Chemistry*, 34(16):1385–1392, 2013. doi: 10.1002/jcc.23271. URL <https://onlinelibrary.wiley.com/doi/abs/10.1002/jcc.23271>.

6 Supplementary Material

6.1 Featurization

We featurize atoms and bonds with one-hot encoded vectors of features calculated using Rdkit [Landrum]. We select features that allow for correct reconstruction of all products and substrates from the development set. In Tables 6 and 7 we present all used features and their possible values found on USPTO-50k. We concatenate one-hot feature vectors to gain the final input representation of atoms and bonds $H^{OH} \in \mathbb{Z}_{\geq 0}^{n \times h_{OH}}$ and $A^{OH} \in \mathbb{Z}_{\geq 0}^{n \times n \times a_{OH}}$. During evaluation, if an unknown feature value is seen (for instance, BOND TYPE=QUADRUPLE), we set the one-hot vector for this feature to zeros. For supernodes, all one-hot feature vectors are set to zeros, apart from vectors for the features IS SUPERNODE and BOND TYPE. We connect each atom with itself with a special bond of type SELF. For non-neighboring atoms at i and j we set $A_{ij}^{OH} = \vec{0}$.

For both atoms and bonds, we add a special IS EDITED feature that marks all bonds and atoms that have been modified by actions. This aims to help the decoder to focus on these atoms and bonds, as they are the most probable candidates for the next generation steps.

6.2 Graph edit actions

In Table 10 we show all possible graph actions found on the USPTO-50k development set. The actions were found during the generation of the training samples, which we describe in the next paragraph. The actions have different sets of parameters, depending on the action type.

For *EditAtom*, the action parameters are the atom properties that are changed by the action. Note that a single *EditAtom* action sets all these properties to the specified values. For instance, action number 1, when executed on an atom, sets its formal charge to 0, chiral tag to None, number of explicit Hydrogen atoms to 1 and marks it as aromatic. *EditBond* acts similarly to *EditAtom* but edits properties of a bond instead of an atom. *AddAtom* adds a new atom with specified features, connected to an existing atom with a bond with specified features. *AddBenzene* appends a benzene ring to a specified carbon atom and has no parameters. *Stop* terminates reaction generation and also has no parameters.

BondEdit actions are bond actions, that is they are predicted for a pair of atoms. All other types of actions are atom actions and are predicted for a single atom in the graph.

6.3 Generating training samples

For each reaction from the development set, we generate training samples by finding actions that lead from the input graph to the target graph. We construct the input graph I and the target graph T using features from Tables 6 and 7. We also initialize the stack of edited atoms $S = \{\}$, which is used for drawing candidate atoms for actions, prioritizing editing already changed atoms. At each step, we execute the first possible action for the concatenated lists of candidate atoms $S \parallel A(I)$, where $A(I)$ is the list of all atoms from the input in randomized order. After each step, we push the modified atoms to the stack S . If there is more than one possible action to perform on a selected atom i or atom pair i, j , we use the following priority of actions II:

- Action that deletes the existing bond between i, j
- Any action that adds a bond between i, j
- Any action that edits the existing bond between i, j
- Any action that edits the existing atom i
- Any action that adds a benzene ring to i

- Any action that adds an atom to i

where bond deletion has the highest priority. The aim is to prioritize actions that are usually the hardest (such as deleting a bond, which usually means finding the reaction center) or logically follow each other (editing a neighboring bond and/or atom often follows bond deletion or addition). For forward synthesis, we use the same priority of actions, except for the first two types of actions which are swapped, so that bond addition (which usually determines reaction center for forward synthesis) has the highest priority. The training reaction generation for the *BFS rand-at* action ordering (see section 4.3.1) is described in Algorithm 1.

6.4 Hyperparameter search

Table 8 shows the hyperparameter values used for the final models. We found them heuristically by observing the validation loss when training on USPTO-50k with unknown reaction type. We tried increasing N_e to 8, as well as K to 12 and h to 1440 but we did not see a decrease in validation error. We also wanted the decoder to be as small as possible, as it is invoked multiple times during the reaction generation. We found that $N_d = 2$ is sufficient to achieve the best accuracy and increasing it lead to faster overfitting. The total number of learnable parameters in the model is approximately 9.9 million.

Table 6: Features of atoms found on USPTO-50k

| NAME | POSSIBLE VALUES | DIM |
|-----------------------|-----------------------------------------------------------|-----|
| IS SUPERNODE | YES, NO | 2 |
| ATOMIC NUMBER | 5, 6, 7, 8, 9, 12, 14, 15, 16, 17, 29, 30, 34, 35, 50, 53 | 16 |
| FORMAL CHARGE | -1, 0, 1 | 3 |
| CHIRAL TAG | NONE, @, @@ | 3 |
| NUMBER OF EXPLICIT HS | 0, 1, 2, 4 | 4 |
| IS AROMATIC | YES, NO | 2 |
| IS EDITED | YES, NO | 2 |
| TOTAL | | 32 |

Table 7: Features of bonds found on USPTO-50k

| NAME | POSSIBLE VALUES | DIM |
|-------------|---------------------------------------------------|-----|
| BOND TYPE | SUPERNODE, SELF, SINGLE, DOUBLE, TRIPLE, AROMATIC | 6 |
| BOND STEREO | NONE, Z, E | 3 |
| IS EDITED | YES, NO | 2 |
| TOTAL | | 11 |

Table 8: Final model hyperparameter values

| h | a | d | K | N_e | N_d | TOTAL PARAMS |
|------|-----|-----|-----|-------|-------|--------------|
| 1024 | 128 | 128 | 8 | 6 | 2 | ~9.9 MIL |

Table 9: datasets information

| | # TRAIN | # VALID | # TEST | # TOTAL | TASK | MAX STEPS | COVERAGE |
|------------|---------|---------|--------|---------|---------|-----------|----------|
| USPTO-50k | 39662 | 5199 | 5155 | 50016 | RETRO | 16 | 99.82% |
| USPTO-FULL | 810496 | 101311 | 101311 | 1013118 | RETRO | 32 | 94.90% |
| USPTO-MIT | 409029 | 30000 | 40000 | 479029 | FORWARD | 8 | 99.99% |

Table 10: Graph actions found on the USPTO-50k development set

| ACTION TYPE | ACTION PARAMETERS | # ACTIONS |
|-------------------|-------------------------------------------------------------------------------------------|-----------|
| <i>EditAtom</i> | FORMAL CHARGE, CHIRAL TAG, NUM OF EXPLICIT HS, IS AROMATIC | 11 |
| <i>EditBond</i> | BOND TYPE, BOND STEREO | 7 |
| <i>AddAtom</i> | ATOMIC NUM, FORMAL CHARGE, CHIRAL TAG, NUM OF EXP HS, IS AROMATIC, BOND TYPE, BOND STEREO | 34 |
| <i>AddBenzene</i> | / | 1 |
| <i>Stop</i> | / | 1 |
| | | 54 |

Algorithm 1 Generating training samples for a reaction (*BFS rand-at* action ordering)

Input: input graph I , target graph T
Initialize $S := \{\}$ (empty list)
Let $A(I) = \{\text{all atoms from } I\}$
marker:
while $I \neq T$ **do**
 shuffle $A(I)$ randomly (for *cano-at*: order $A(I)$ by map numbers)
 for i in $S \parallel A(I)$ **do**
 for P in Π **do**
 for a in P **do**
 if a is an atom action **then**
 if applying a to i leads to T **then**
 generate training sample $(I, a(i))$
 apply action a to atom i in I
 $S := S \parallel \{i\}$ (for *DFS*: $S := \{i\} \parallel S$)
 go to marker
 end if
 else if a is a bond action **then**
 for j in $S \parallel A(I)$ **do**
 if applying a to i, j leads to T **then**
 generate training sample $(I, a(i, j))$
 apply action a to atoms i, j in I
 $S := S \parallel \{i, j\}$ (for *DFS*: $S := \{j, i\} \parallel S$)
 go to marker
 end if
 end for
 end if
 end for
 end for
 end for
 end for
end while
